IOPscience iopscience.iop.org

Home Search Collections Journals About Contact us My IOPscience

The structural, optical and electrical properties of Y-doped SnO thin films and their p-type TFT application

This article has been downloaded from IOPscience. Please scroll down to see the full text article.

2012 J. Phys. D: Appl. Phys. 45 085101

(http://iopscience.iop.org/0022-3727/45/8/085101)

View the table of contents for this issue, or go to the journal homepage for more

Download details:
IP Address: 210.72.19.250
The article was downloaded on 09/02/2012 at 11:40

Please note that terms and conditions apply.

J. Phys. D: Appl. Phys. **45** (2012) 085101 (5pp) doi:10.1088/0022-3727/45/8/085101

The structural, optical and electrical properties of Y-doped SnO thin films and their p-type TFT application

Ling Yan Liang, Zhi Min Liu, Hong Tao Cao, Wang Ying Xu, Xi Lian Sun, Hao Luo and Kai Cang

Ningbo Institute of Materials Technology and Engineering (NIMTE), Chinese Academy of Sciences (CAS), Ningbo 315201, People's Republic of China

E-mail: H_cao@nimte.ac.cn

Received 30 October 2011, in final form 27 December 2011
Published 9 February 2012
Online at stacks.iop.org/JPhysD/45/085101

Abstract
Unintentionally doped and Y-doped SnO thin films were prepared and characterized by x-ray diffraction, spectroscopic ellipsometry, and Hall-effect measurements. SnO-based thin-film transistors were also fabricated and investigated. Preferred $(0\,0\,l)$ grain orientation present in the undoped films is alleviated by Y doping, inducing the deterioration of crystallinity as well as the decrease in Hall-effect and saturation field-effect mobilities. However, both the films and the transistor devices always possess p-type characteristics in this study. As the Y content increases, the optical band gap, the real part of the dielectric constant of the films and the on/off current ratio of the devices increase. Moreover, the threshold voltage was observed to shift towards the positive direction as more yttrium content is introduced. These results give evidence that the yttrium element is incorporated into the SnO lattice successfully and higher hole concentration can be generated.

(Some figures may appear in colour only in the online journal)

1. Introduction

Tin monoxide (SnO) has been studied as the anode material [1], gas sensitive material [2], coating substance [3], catalyst [3], precursor for the production of tin oxide (SnO_2) [4] and semiconductor layer for p-channel thin-film transistors (TFTs) [5–7]. TFTs employing SnO channels have exhibited to date the highest field-effect mobility ($\sim 1\,cm^2\,V^{-1}\,s^{-1}$) among the reported values for p-channel oxide TFTs [8]. Moreover, oxide semiconductor-based complementary metal-oxide-semiconductor (CMOS) inverters have been reported using gallium–indium–zinc oxide and non-stoichiometric tin oxide (SnO_x, $x < 2$) as the channel layers [9].

Although SnO film has received increasing attention, there are only a few reports focusing on the effects of doping on its physical properties. It is reported that dopants can be incorporated into the SnO crystal lattice, but the microscopic doping mechanism has not been demonstrated yet [10–12]. Guo *et al* speculated that the charge defect complexes $(Sb_{Sn} - 2V_{Sn})^-$ act as the acceptor when large size dopants such as Sb (or Y) are introduced into SnO [11]. They reported that doping of Y^{3+} or Sb^{3+} up to 5 at% into SnO can further enhance the p-type conduction according to the Hall-effect measurements. However, the above speculation is conflicted with the results of Hosono *et al* [12]. They provided clear evidence of n-type behavior in the Sb-doped SnO by Hall-effect measurement, thermopower observation and the signature from SnO p/n junction. So far, the effect of Y-element doping on the conduction of SnO films is not clear, and thus is worth studying in more detail. Moreover, the dependence of the structural and optical properties of SnO thin films on foreign element doping, which is essential to understand the electrical transport properties, has rarely been investigated up to now.

In this work, we studied the microstructural, optical and electrical properties of both unintentionally doped and yttrium (Y)-doped SnO thin films grown on Si substrates (with SiO_2 overcoat) by electron-beam evaporation (EBE). It was found that the introduction of yttrium element resulted in higher hole concentration. Furthermore, TFTs using the obtained films as channels were fabricated, and the influence of Y doping on

 © 2012 IOP Publishing Ltd Printed in the UK & the USA

their electrical properties was also analysed, which confirms the p-type behavior.

2. Experiment details

Unintentionally doped and Y-doped SnO thin films were deposited by EBE on Si substrates (with SiO_2 layers of 190 nm). A series of well sintered SnO_2 ceramics as EBE precursors with Y : (Y + Sn) atomic ratio in the range 0–13% were obtained from $Sn(CO_3)_2$ and $Y_2(CO_3)_3$ mixed powders by conventional sintering method. Thin films were deposited at room temperature (RT) with a rate of about 3.6 nm min^{-1}. The detailed description of the experimental procedure can be found in [13]. Then the films were subjected to thermal annealing at 350 °C for 3 h in a vacuum chamber with a base pressure of 2.0×10^{-4} Pa for the purpose of crystallization. The crystal structures of the films were examined by x-ray diffraction (XRD) in the symmetric-reflection-coupled θ–2θ arrangement. XRD patterns were recorded on a Bruker D8 Advance x-ray diffractometer using Cu K_α radiation ($\lambda_0 = 1.5418$ Å). The thicknesses and optical properties of the films were analysed via a variable angle spectroscopic ellipsometer (SE, J.A.Woollam Inc.). The yttrium doping level in the bulk ceramics and thin films were determined by x-ray photoemission spectroscopy (XPS, Kratos Analytical Ltd, UK) equipped with a standard monochromatic Al-K_α source ($h\nu = 1486.6$ eV). High dose of argon ions was used to sputter away the top hydrated and carbon contamination layer (2–3 nm) of the films. The Y : (Y + Sn) atomic ratios were about 0.4% and 0.8% in the films corresponding to the nominal values of 8 at% and 13 at% in the source materials, respectively. It is noted that the real Y concentrations in the films deviated largely from those in the EBE precursors, which is consistent with the previous report [12].

Bottom-gate type TFTs were fabricated using 50 nm thick films (patterned by the first shadow mask) as channels, heavily doped p-type silicon as substrate and gate electrode, and thermally oxidized 190 nm thick SiO_2 layer as gate dielectric (the gate capacitance per unit area $C_0 = 17$ nF cm^{-2}). Ni/Au (30 nm/50 nm) contact pads were evaporated on the top of the channel layers through the second shadow mask at RT by EBE. The length (L) and width (W) of the channels were 100 μm and 1000 μm, respectively. The electrical properties of the channels were studied by Hall-effect measurement system (ACCENT, HL5500). Device characteristics of SnO-TFTs were measured at RT using a Keithley 4200 Semiconductor Parameter Analyzer and SÜSS PM5 probe station. All measurements were carried out in the dark to avoid photo-generated effects.

3. Results and discussion

Figure 1 presents XRD patterns of the films with different Y contents. All of the diffraction peaks correspond to the reflections of the α-SnO phase (labelled with α, tetragonal litharge structure, JCPDS card No 06-0395), and no peaks related to other phases were detected. The unintentionally doped ones exhibited strong preferred orientation of (0 0 l),

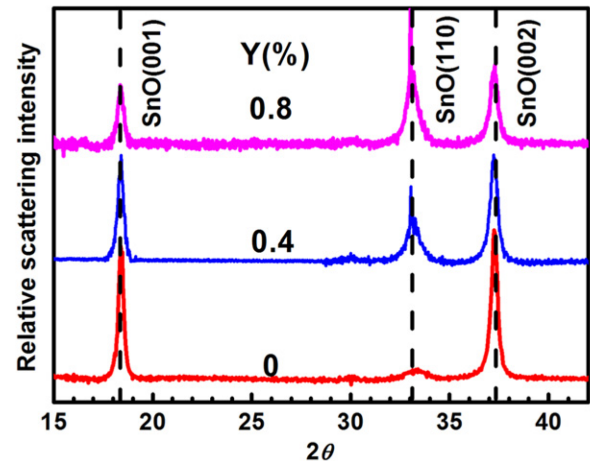

Figure 1. XRD patterns of the unintentionally doped and Y-doped SnO films. The background has been subtracted for clarity.

which is similar to the reported results [11]. With increasing Y content, the full width at half maximum (FWHM) of the (0 0 l) peak increased in conjunction with the tapered (0 0 l) peak intensity, while the (1 1 0) peak intensity increased concomitantly, indicating the presence of more random orientation and worse crystallinity caused by the foreign doping. The deterioration of crystallinity, i.e. the increase in the inhomogeneous strain in the films and/or the reduction in the average grain size (i.e. higher grain boundary density), could lead to prominent carrier scattering during transportation. Herein, it is speculated that the electrical properties of both the films and the TFT devices would change a lot resultantly since the electrical transport properties are coupling well with the film quality.

By virtue of the spectroscopic ellipsometry method, the influence of Y doping on the optical constants of SnO films was also investigated. A simple four-phase model consisting of Si substrate/SiO_2 film/Y-doped SnO thin film/surface rough layer (50% Y-doped SnO + 50% void) was used to represent the sample. Two Tauc–Lorentz (TL) dispersion functions were employed to characterize the dielectric function of the Y-doped SnO films. The fitting procedure can be found elsewhere [14]. Meanwhile the refractive index n and extinction coefficient k can be obtained according to their relationship with the real and imaginary part of the dielectric constant (ε_1, ε_2) [15].

As depicted in figure 2, the imaginary part (ε_2) of the dielectric constant of the unintentionally doped SnO thin film shows a strong peak at around 342 nm (3.62 eV) due to interband transitions, or more concretely, due to the optical transitions from the valence band to the lowest part of the conduction band. The peak position blue-shifts to 335 nm (3.70 eV) and the peak amplitude increases as Y element is incorporated into the films. The real part (ε_1) of the dielectric constant also presents a strong peak, and the peak position shifts from 396 to 366 nm as the Y concentration increases from 0 to 0.8 at%. In particular, the ε_1 value at the wavelength (λ) above 400 nm (the visible and near infrared regions) becomes bigger and bigger with increasing Y content, as shown in table 1. The increment of ε_1 is ascribed to the increase in the refractive index n, since ε_1 is roughly equal to n^2 in the visible

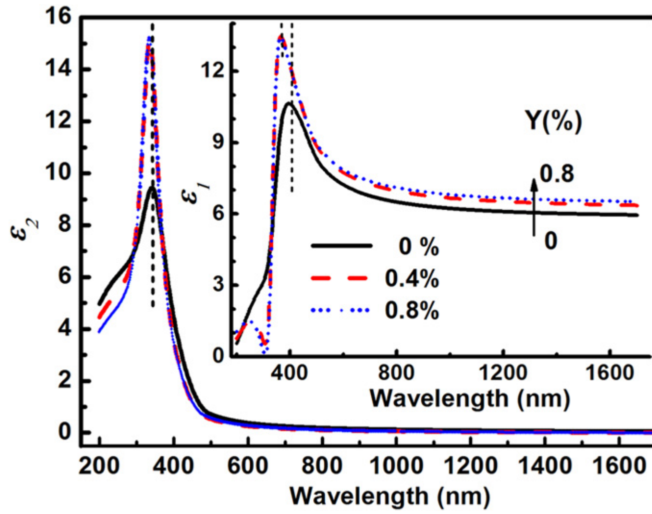

Figure 2. Spectroscopic ellipsometry spectra of the imaginary part ε_2 and real part ε_1 (the inset) of the dielectric constants of SnO films with different Y contents.

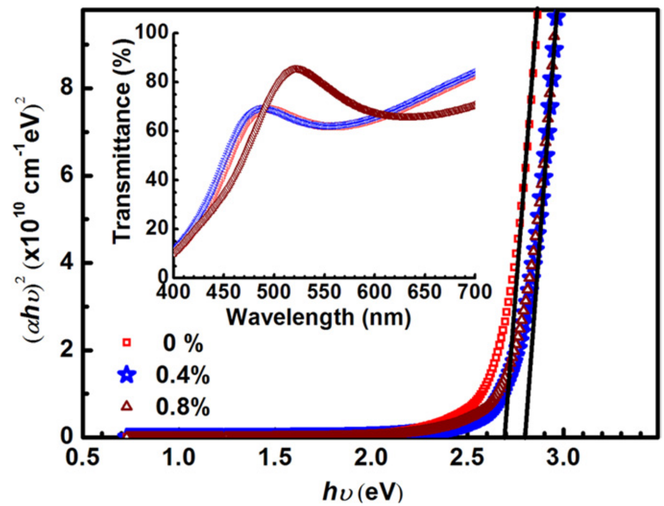

Figure 3. Plots of $(\alpha h\upsilon)^2$ versus $h\upsilon$ for the SnO films with different Y contents. The inset is the transmittance curve.

Table 1. The ε_1 value at $\lambda = 1700$ nm, the optical band gap E_g and the averaged transparency T of the thin films with different Y contents.

Y (at%)	0	0.4	0.8
ε_1 (n^2)	5.95	6.36	6.52
E_g (eV)	2.70	2.80	2.80
T(%)	60	61	61

and near infrared regions in which the extinction coefficient k of all the obtained films is very small or close to zero. The n values at $\lambda > 400$ nm of Y_2O_3 are far smaller than those of SnO. For example, the n value of Y_2O_3 is less than 1.9 at 1700 nm [16–18], while that of the undoped SnO film is around 2.43. From the above comparison, the simple mixture of Y_2O_3 and SnO phases could not lead to the increase in the n value, so it is inferred exclusively that the trace content of yttrium was incorporated into the SnO lattice successfully, which is responsible for the increased n value.

The optical band gap (E_g) can be calculated using the following equation:

$$(\alpha h\upsilon)^2 = A(h\upsilon - E_g), \quad (1)$$

where A is a constant, $h\upsilon$ the photon energy and α the absorption coefficient that can be calculated via $\alpha = 4\pi k/\lambda$. Figure 3 exhibits the $(\alpha h\upsilon)^2$ versus $h\upsilon$ plots for the films. The calculated E_g values are listed in table 1. In accordance with the blue-shift of the dielectric constant peak, the optical band gap also exhibits a blue-shift of about 0.10 eV as the Y concentration increases from 0 to 0.8 at%. Thin films were also deposited on quartz glass for acquiring the transmittance, as displayed in the inset of figure 3. All films feature a yellowish colour with an average optical transparency of 60–61% in the visible regions ($\lambda = 400$–700 nm).

Electrical properties of the obtained films were examined by the Hall-effect measurement, as listed in table 2. It is shown that the hole concentration increases from 5.6×10^{15} to 4.7×10^{16} cm^{-3} but the Hall mobility decreases from 3.9 to 0.8 cm^2 V^{-1} s^{-1} as the Y content increases from 0 to 0.8 at%. The Hall mobility decreasing trend with Y content is opposite to the report in [11], which is partially due to the different preparation conditions (RT deposition and post-annealing in this study, but *in situ* deposition at 350 °C in [11]). But most importantly, the decrease in the mobility in this study is believed to be caused by the deterioration of crystallinity according to the XRD results.

Figures 4(*a*)–(*c*) depict the output characteristics of the TFTs using the SnO thin films with different Y contents as the channels. It can be seen that all the devices exhibit p-type field-effect transistor characteristics, i.e. negative gate bias V_G increases drain–source current $|I_{DS}|$ conspicuously. The transfer curves of the studied devices are illustrated in figures 4(*d*)–(*f*). The electrical parameters can be obtained from the transfer curves, as summarized in table 2. The turn-on voltage V_{on} is defined as the gate voltage at which $|I_{DS}|$ begins to increase in a transfer curve. The saturation mobility (μ_{sat}) is calculated using the following relations: $\mu_{sat} = 2LI_{DS}/WC_0(V_G - V_{th})^2$, in which V_{DS}, and V_{th} are the drain bias and threshold voltage, respectively. The V_{th} is estimated from the $(-I_{DS})^{1/2}$ versus V_G plots.

From table 2, V_{on} turns from negative to positive when the Y-doped films are served as the channel, and becomes more positive with doping level. Theoretically, V_{on} is a 'watershed' voltage at which the state of the channel turns from accumulation to depletion, so the V_{on} value is related to the conduction type and intrinsic carrier concentration in the channel, i.e. a larger positive voltage is necessary to deplete a channel with a higher hole concentration [19]. The variation of the V_{on} value is consistent with the increase in the hole concentration with Y content in the channels according to the Hall-effect measurement. The V_{th} is also observed to shift towards the positive direction with increasing Y contents, agreeing fairly well with the variation trend of V_{on}. The saturation field-effect mobility μ_{sat}, however, decreases with increasing Y content, which can be reminiscent of the aforementioned deteriorated crystallinity as well as the variation of Hall mobility. The off current I_{off} of the

Table 2. The hole concentration (N_{Hall}), hole mobility (μ_{Hall}) and resistivity (ρ) of the obtained films by the Hall-effect measurement, and the electrical parameters of the TFTs using the films as channels.

Y (at%)	N_{Hall} (10^{16} cm^{-3})	μ_{Hall} (cm^2 V^{-1} s^{-1})	ρ (Ω cm)	V_{on} (V)	V_{th} (V)	I_{on}/I_{off}	I_{off} (nA)	μ_{sat} (cm^2 V^{-1} s^{-1})
0	0.56	3.9	280	−7	−20.5	90	∼500	0.16
0.4	1.5	2.9	133	1.5	−15	260	∼17	0.012
0.8	4.7	0.8	120	14	−13	400	∼3.8	0.0036

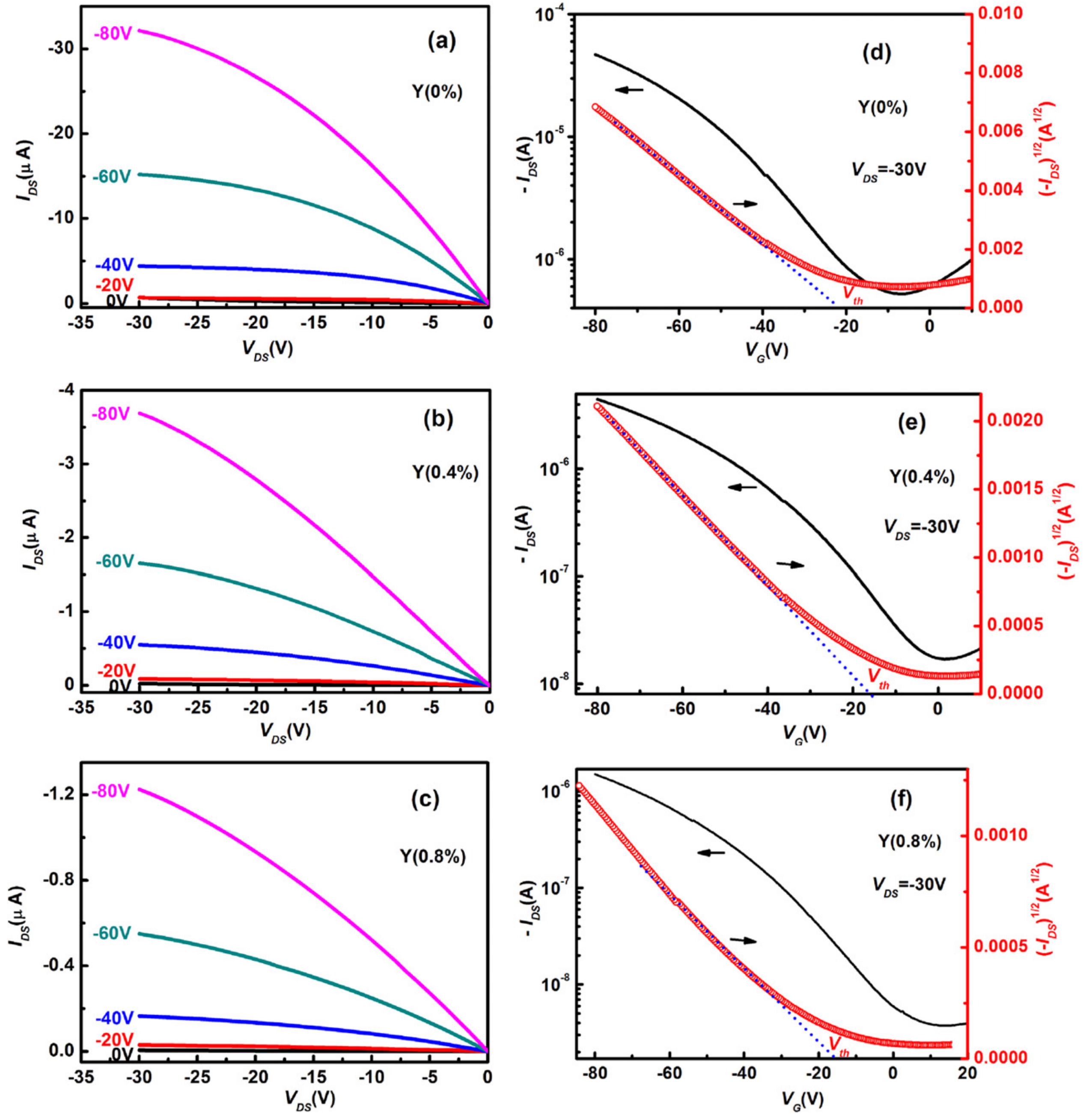

Figure 4. Output (a)–(c) and transfer (d)–(f) curves of the TFTs using SnO thin films with different Y contents as the channels. The dot lines were plotted to obtain the threshold voltage V_{th}.

unintentionally doped SnO-TFT is a bit high (∼500 nA), as reported previously [6, 20]. But interestingly, I_{off} of the Y-doped SnO-TFTs reduces largely, leading to an obvious increase in the on/off current ratio I_{on}/I_{off}. It is reported that the possible origin of the high off current in SnO-TFTs lies in the fact that too many extra trap states exist at the deep energy levels (>0.2 eV above the valence band) and the Fermi level can not be raised by applying larger positive V_G [6, 20]. In this study, the exact reason for the reduction in I_{off} is unknown and under investigation.

4. Conclusions

Unintentionally doped and Y-doped SnO thin films were prepared from SnO_2 source with different Y contents via electron beam evaporation and vacuum annealing. SnO-based TFTs were also fabricated and investigated. According to the XRD results, preferred $(0\,0\,l)$ orientation is present in the unintentionally doped films and then alleviated by Y doping, which results in the deterioration of crystallinity. Both the optical band gap and real part of the dielectric constant of the film increase with Y content by spectroscopic ellipsometry analysis. All the thin films and devices feature the p-type characteristics. As the Y content increases, on the one hand, the turn-on voltage changes from negative to positive and the negative threshold voltage shifts towards the positive direction, which is related to more hole concentration in the semiconductor layer; on the other hand, both the Hall mobility and saturation field-effect mobility decrease due to the deterioration of the film crystallinity. In particular, the on/off current ratio is improved by Y doping, stemming from the lower off current.

Acknowledgments

The authors are grateful for the financial support of the National Natural Science Foundation of China (Grant Nos 61076081 and 11104289), the Natural Science Foundation of Ningbo (Grant No 2010A610182), the National Program on Key Basic Research Project (2012CB933000), the aided program for Science and Technology Innovative Research Team of Ningbo Municipality (2009B21005), and the key program for Science and Technology Innovative Team of Zhejiang Province (2010R50020).

References

[1] Ning J J, Jiang T, Men K K, Dai Q Q, Li D M, Wei Y J, Liu B B, Chen G, Zou B and Zou G T 2009 *J. Phys. Chem.* C **113** 14140

[2] Calderer J, Molinas P, Sueiras J, Llobet E, Vilanova X, Correig X, Masana F and Rodriguez A 2000 *Microelectron. Reliab.* **40** 807

[3] Giefers H, Porsch F and Wortmann G 2005 *Solid State Ion.* **176** 199

[4] Pan X Q and Fu L 2001 *J. Appl. Phys.* **89** 6048

[5] Ogo Y, Hiramatsu H, Nomura K, Yanagi H, Kamiya T, Hirano M and Hosono H 2008 *Appl. Phys. Lett.* **93** 032113

[6] Liang L Y, Liu Z M, Cao H T, Yu Z, Shi Y Y, Chen A H, Zhang H Z, Fang Y Q and Sun X L 2010 *J. Electrochem. Soc.* **157** H598

[7] Fortunato E, Barros R, Barquinha P, Figueiredo V, Park S H K, Elamurugu E, Hwang C S and Martins R 2010 *Appl. Phys. Lett.* **97** 052105

[8] Matsuzaki K, Nomura K, Yanagi H, Kamiya T, Hirano M and Hosono H 2009 *Phys. Status Solidi* a **206** 2192

[9] Martins R, Nathan A, Barros R, Pereira L, Barquinha P, Correia N, Costa R, Ahnood A, Ferreira I and Fortunato E 2011 *Adv. Mater.* **23** 4491

[10] Xu C, Tamaki J, Miura N and Yamazoe N 1992 *J. Mater. Sci.* **27** 963

[11] Guo W, Fu L, Zhang Y, Zhang K, Graham G, Liang L Y, Liu Z M, Cao H T and Pan X Q 2010 *Appl. Phys. Lett.* **96** 042113

[12] Hosono H, Ogo Y, Yanagi H and Kamiya T 2011 *Electrochem. Solid-State Lett.* **14** H13

[13] Liang L Y, Liu Z M, Cao H T and Pan X Q 2010 *ACS Appl. Mater. Interfaces* **2** 1060

[14] Liang L Y, Liu Z M, Cao H T, Shi Y Y, Sun X L, Yu Z, Chen A H, Zhang H Z and Fang Y Q 2010 *ACS Appl. Mater. Interfaces* **2** 1565

[15] Pan S S, Zhang Y X, Teng X M, Li G H and Li L 2008 *J. Appl. Phys.* **103** 093103

[16] Rouffignac P, Park J S and Gordon R G 2005 *Chem. Mater.* **17** 4808

[17] Wang X J, Zhang L D, Zhang J P, He G, Liu M and Zhu L Q 2008 *Mater. Lett.* **62** 4235

[18] Zhang H Z, Liang L Y, Chen A H, Liu Z M, Yu Z, Cao H T and Wan Q 2010 *Appl. Phys. Lett.* **97** 122108

[19] Wager J F, Keszler D A and Presley R E 2008 *Transparent Electronics* 1st edn (New York: Springer) p 109

[20] Ogo Y, Hiramatsu H, Nomura K, Yanagi H, Kamiya T, Kimura M, Hirano M and Hosono H 2009 *Phys. Status Solidi* a **206** 2187